Appl. Phys. A (2017) 123:670
DOI 10.1007/s00339-017-1282-x

Applied Physics A
Materials Science & Processing

Production of precursors for micro-concentrator solar cells by femtosecond laser-induced forward transfer

Stefan Andree[1] · Berit Heidmann[2,3] · Franziska Ringleb[4] · Katharina Eylers[4] · Jörn Bonse[1] · Torsten Boeck[4] · Martina Schmid[2,3] · Jörg Krüger[1]

Received: 30 June 2017 / Accepted: 22 September 2017

Abstract Single-pulse femtosecond laser-induced forward transfer (LIFT, 30 fs, 790 nm) is used to deposit micron-sized dots of copper and/or indium onto a molybdenum layer on glass. Such systems can serve as precursors for the bottom–up manufacturing of micro-concentrator solar cells based on copper–indium–gallium–diselenide. The influence of the thickness of the copper, indium, and combined copper–indium donor layers on the quality of the transferred dots was qualified by scanning electron microscopy, energy-dispersive X-ray analysis, and optical microscopy. The potential for manufacturing of a spatial arrangement adapted to the geometry of micro-lens arrays needed for micro-concentrator solar cells is demonstrated.

1 Introduction

During the past years, significantly increasing research activities in the field of novel concepts for photovoltaics were reported [1, 2]. One promising approach is based on micro-concentrator solar cells, where the photovoltaic active area is realized as an array of sub-millimeter sized thin-film solar cells, arranged each in the focus of one lens of a regular arrangement of micro-lenses. The micro-concentrator methodology combines the potential for a significant material saving of solar cell compounds (e.g., rare elements such as indium) with a beneficial heat management and allows to increase the solar cell efficiency under concentrated illumination [3, 4]. Figure 1 provides a scheme of a micro-solar cell arrangement consisting of a glass substrate covered by a molybdenum back contact, with a CIGSe solar absorber, a CdS buffer layer, and a ZnO front contact.

Given the current record efficiencies of $> 22\%$ for planar thin-film $CuInGaSe_2$ (CIGSe) solar cells, this material system appears very promising for micro-concentrator applications [5]. For the manufacturing of micro-concentrator cells, a material saving arrangement of the micro-sized solar absorber is desired. Therefore, a laser-based processing in a bottom–up procedure is favorable, since the laser allows a contactless and site-selective modification of bulk and thin-film materials. In a previous work, a fs-laser-induced roughening of the molybdenum back contact for a site-selective aggregation of indium droplets during subsequent physical vapor deposition (PVD) was used [6]. Additional postprocessing involved the PVD of copper followed by selenization. This finally leads to CIGSe micro-solar cells [7].

However, to reduce the number of process steps in the manufacturing of micro-concentrator solar cells, the site-specific direct transfer of the solar absorber (CIGSe) precursor material with the desired dimensions would be beneficial. In principle, the technique laser-induced forward transfer (LIFT) fulfils all these requirements [8–22]. In this LIFT technique, a single laser pulse is focused through a glass substrate coated with a donor layer. For suitably chosen conditions (peak fluence, pulse duration, focussing, etc.), a part of the donor layer is selectively

✉ Jörg Krüger
joerg.krueger@bam.de

[1] Bundesanstalt für Materialforschung und -prüfung (BAM), Unter den Eichen 87, 12205 Berlin, Germany

[2] Helmholtz-Zentrum Berlin für Materialien und Energie, Hahn-Meitner-Platz 1, 14109 Berlin, Germany

[3] Fakultät für Physik, Universität Duisburg-Essen und CENIDE, Lotharstr. 1, 47057 Duisburg, Germany

[4] Leibniz-Institut für Kristallzüchtung, Max-Born-Str. 2, 12489 Berlin, Germany

Published online: 30 September 2017

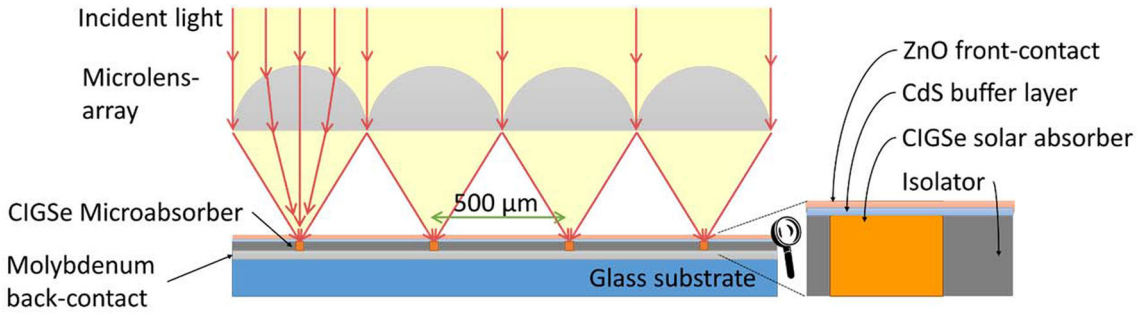

Fig. 1 Copper–indium–gallium–diselenide (CIGSe) micro-concentrator solar cell design

removed from the donor glass substrate and transferred to the receiver substrate (see the scheme in Fig. 2). For manufacturing of micro-concentrator solar cells via LIFT, the receiver may consist of a glass substrate fully covered by a molybdenum back contact. Upon moving the entire donor–acceptor arrangement transversely under the laser beam, regular arrays of sub-mm-sized dots of the donor layer can be directly written onto the receiver. LIFT represents a powerful and flexible technique that is capable to transfer solid layers as well as liquids (such as functionalized inks including complex materials) [8, 11, 15–17], entire organic thin-film transistors [9, 19], or even living biological cells [20] and other biomaterials [22].

It is important to underline the requirements which are imposed to the LIFT process for the manufacturing of micro-concentrator solar cells: (1) a successful transfer of 10–60 µm diameter discs of indium and/or copper material with a height-to-diameter aspect ratio between 0.01 and 0.1 is desired. (2) The material should be transferred by a single laser pulse. As a consequence, donor and acceptor can be moved synchronously, which simplifies the experimental setup. (3) The transferred disc should show a sharp boundary and a homogeneous coverage on the acceptor.

Several groups have already studied the deposition of metal films via LIFT [12, 23, 24] and particularly metals used in CIGSe solar cells, such as copper [25, 26, 30–32] and indium [27–29]. Some references describe the LIFT-based assembly of larger 2D/3D structures from a sequence of micrometer-sized single transfers. For example, Zenou et al. [31, 32] demonstrated the bottom–up manufacturing of copper structures with characteristic lengths from 10 µm to several 100 µm from a sequence of dots having 6.5 µm diameter and 600 nm height using sub-nanosecond pulses.

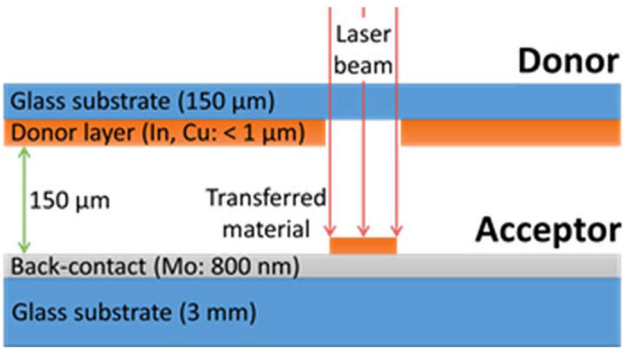

Fig. 2 Scheme of the laser-induced forward transfer (LIFT) indicating thicknesses of donor and acceptor components

With picosecond laser pulses at 515 nm wavelength, Visser et al. created copper pillars with an aspect ratio of 16 having 80 µm height and 5 µm diameter [33]. Pohl et al. identified different regimes for ps-LIFT with increasing fluence: for low fluence, no ejection is observed, followed by the release of a metal cap (i.e., a hemisphere-shaped droplet), the formation of an elongated jet, and for high fluences, the release of a metal spray [26].

In the femtosecond regime, the assembly of copper wires from overlapping disc-shaped transferred material was described by Grant-Jakob et al. using 150 fs pulses with 800 nm wavelength and 1 kHz repetition rate [25]. These wires with a length of several hundred micrometers had rectangular cross sections with widths and heights in the range 1–3 µm and an aspect ratio near one. Alti et al. and Thomas et al. reported high repetition rate laser-written line structures consisting of indium with 50 fs pulses, 800 nm wavelength, and 5 MHz repetition rate [27, 28]. Due to the large repetition rate, the wire was composed of millions of single transfers and the best quality was achieved for aspect ratios near one. Single micro-droplets of copper with diameters of 2–20 µm were transferred by Yang et al. and Li et al. (150 fs single pulses, 780 nm, 3.2 J/cm^2) [29, 30]. These droplets varied from a Gaussian to a donut-shaped profile as determined by AFM images. For intermediate profiles (with a strong height variation), a height-to-diameter aspect ratio of about 0.1 was observed. However, their diameters were smaller than required for the micro-solar cell application. Hence, the results on LIFT of precursor materials for CIGSe solar cells available in the literature do not meet the mentioned requirements (1)–(3).

In this work, we provide a proof-of-principle that micro-sized precursor materials for CIGSe solar cells can be transferred via femtosecond LIFT to a molybdenum back-

contact layer. This is realized by single-pulse transfer using short pulse durations (∼ 30 fs) and large focused beam diameters (∼ 150 µm). It includes a study of individual transfer steps of single metal layers (In, Cu). In addition, it will be shown that metallic multilayers consisting of copper and indium are advantageous in the LIFT processing compared to single layers.

2 Experimental

The experiments were performed using a commercial Ti:Sapphire laser system (Femtolasers Compact Pro). The laser was operated at 30 fs pulse duration and 800 nm center wavelength. Single pulses were selected by gating the laser electronics. The collimated output beam of the femtosecond laser was directed onto the sample by means of a spherical mirror with a focal length of 50 cm. The focused beam radii ($1/e^2$) were determined by a beam analyzer to be 60 and 80 µm in the meridional and sagittal planes, indicating an elliptical beam profile having an aspect of 1.3.

The LIFT samples serving as donors (Fig. 2) were prepared by physical vapor deposition (PVD) of indium and/or copper layers on 150 µm-thick glass slides (borosilicate glass, Weidner Glas). Prior to the PVD process, ultrasonic cleaning of the substrate with acetone, rinsing with isopropanol, ethanol and water as well as drying in nitrogen atmosphere was done. Deposition took place under vacuum (2×10^{-5} mbar) at room temperature with a deposition rate of 1 Å/s for copper and 5 Å/s for indium. For combined copper–indium layers, the copper was deposited first, since copper has a higher melting point. Subsequently, indium was added with thicknesses typically 10–100 times larger than the copper layer thickness. In this way, the more tensile copper (tensile strength: 220 MPa [34]) stabilizes the easily fragmentable indium (tensile strength: 1.6 MPa [35]) during the laser process. The acceptor consisted of a 3 mm-thick float glass substrate PVD-coated with molybdenum of a thickness of 800 nm. For LIFT, the donor and acceptor were aligned parallel and fixed at 150 µm separation with microscope cover plates as spacers.

To optimize the parameters for the LIFT process, several sets of samples were prepared. Copper layers with thicknesses varying from 10 to 100 nm and indium layers varying from 150 to 1000 nm thickness were deposited on glass. In addition, copper–indium layers were produced with (1) varying indium thickness from 200 to 1000 nm coated on 10 nm-thick copper films and (2) varying copper thickness (10–60 nm) for a subsequent coating with constant indium thicknesses of either 200 or 500 nm.

While the copper film shows a mirror-like reflection, the indium samples appear grey and less reflective to the eye, indicating optical scattering through a granular structure of the indium film. The matte surface is also found for the combined copper–indium films. Upon visual inspection through the glass support from the rear side, no pure copper-like reflection is visible. This indicates that copper and indium have formed alloys directly during/after coating and that the type of the alloy varies with the ratio of copper and indium thickness according to the stoichiometric ratios of several Cu–In alloys [36].

For each sample, nine sites were irradiated at different pulse energies ranging from 20 to 200 µJ corresponding to peak fluences of 0.78–7.8 J/cm^2. Using optical microscopy, the areas of the processed donor sites were determined, enabling the calculation of the fluences according to a formalism proposed by Liu [37] and extended to elliptical beam profiles in [38]. That method simultaneously provides the beam diameters and the thresholds for the onset of (LIFT) material removal. They account to 0.26 J/cm^2 for a 150 nm-thick indium film, and 0.3 J/cm^2 for a combined layer consisting of 10 nm copper and 200 nm indium, respectively. The samples were characterized by optical microscopy (OM) and scanning electron microscopy (SEM) combined with energy-dispersive X-ray analysis (EDX).

3 Results and discussion

3.1 LIFT of pure copper films

In a first step, LIFT of pure copper was studied. The copper films (donors) were irradiated by single laser pulses with fluences ranging from 0.78–7.8 J/cm^2. Some optical micrographs of LIFT-processed sites are compiled in Fig. 3 employing a constant energy density of 7.8 J/cm^2 for different copper film thicknesses. The upper row depicts the laser-irradiated donor layer, while the lower row visualizes the corresponding transferred material on the acceptor side. The donor layer thickness is indicated for each pair of donor/acceptor at the bottom of the figure. For a film thickness of 10 nm, the largest removed area on the donor site was obtained, which reflects a reduction of the LIFT threshold with decreasing film thickness. On the corresponding acceptor site, transferred copper material manifests itself as a colorized annulus surrounding the copper-free central region. The annulus is formed by sub-micrometer-sized copper particles. Within the annulus, residuals of molten and solidified material of the receiving molybdenum layer can be observed. The melting originates from a substantial part of the laser pulse (50% linear transmission for a 10 nm-thick copper layer with a copper absorption coefficient of $\alpha = 7.9 \times 10^5$/cm at 800 nm wavelength [39]) being transmitted through the thin copper

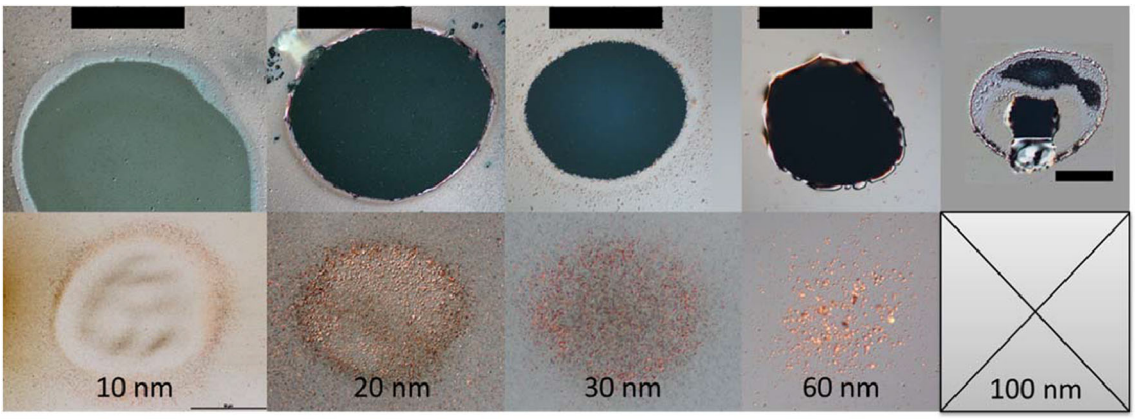

Fig. 3 Optical micrographs of LIFT of copper films for a constant laser fluence of 7.8 J/cm^2. Upper row: laser-irradiated donor layer. Lower row: transferred material on the acceptor side. The copper film thickness is specified. Scalebars correspond to 100 µm (rightmost 50 µm)

layer. It is subsequently absorbed by the molybdenum. The absence of redeposited copper particles in the center of the donor may indicate their incorporation in the molten acceptor (Mo) layer.

For a larger copper film thickness of 20 nm, no indications of transient melting of molybdenum can be seen (linear transmission of 25%). The copper on the acceptor is distributed over the central region, but an annulus with higher copper concentration is still visible. A fraction of the copper particles has a size of a few microns (up to 2.5 µm), as measured by the optical microscope, but there are still many smaller particles in between. For the 30 nm-thick copper layer (linear transmission of 12%), an annulus of transferred copper on the acceptor is not visible. The fractionation in particles is comparable to the case of 20 nm film thickness. For the 60 nm-thick copper film (linear transmission of 1%), the copper concentration is highest in the center of the acceptor and decreases radially. Particle sizes of up to 4 µm and a reduced particle density are observed. An irregular rim surrounding the ablated region of the donor layer is seen. For the 100 nm-thick copper layer, the transmission is 0.1% and no transfer was obtained. This behavior can be understood in terms of the optical penetration depth of the laser pulses into the copper layer. From the linear absorption coefficient α at 800 nm wavelength, a penetration depth $1/\alpha$ of about 13 nm is calculated. Therefore, the excitation condition depends on the film thickness. For the thinnest films (10, 20 nm), the energy is absorbed over the entire layer. This explains the (almost homogeneous) disintegration of the 10 nm donor film into small particles. The finding is supported by femtosecond laser ablation experiments on bulk copper [40] and molecular dynamics simulations of laser interaction with ultrathin metal films [41]. For thicker films (> 30 nm), the pulse energy is essentially deposited at the glass–copper interface of the donor, resulting in an incompletely excited film. Therefore, the film can be delaminated and disintegrates into larger fragments (see copper film thickness of 60 nm). The trend of smaller deposited particles for thinner donor films confirms the results of Rouleau et al. They attribute the smaller fragments to a spallation layer, while the larger particles arise from a region underneath [41]. The copper layer with the highest thickness of 100 nm cannot be transferred, since it rather partially delaminates than disintegrates into particles.

Figure 4 summarizes LIFT transfer results of copper donor layers on the acceptor. The peak fluence varies from the top to the bottom, while the copper donor film thickness increases from left to right. For donor film thicknesses up to 30 nm, the peak fluence mainly changes the area of the deposited material, as it can be expected for a threshold-driven process. For the film thickness of 60 nm, the deposited size of the copper is almost independent on the laser fluence. As discussed in the context of Fig. 3, the delamination and disintegration into larger fragments of an incompletely excited film are seen here too.

3.2 LIFT of pure indium films

In contrast to copper films, indium can be transferred also from donors of larger layer thicknesses. Supposedly, this arises from a different film quality (closed copper films vs. granular indium layers) and varying thermo-physical properties of the materials. Exemplifying optical micrographs are given for a LIFT donor with a 150 nm-thick indium layer (Fig. 5, left), the corresponding transferred material on the acceptor (Fig. 5, middle), and the transferred material obtained from a 300 nm-thick indium donor layer (Fig. 5, right)—all irradiated at identical conditions (7.8 J/cm^2). That fluence is more than one order of magnitude larger than the LIFT threshold of a 150 nm-thick

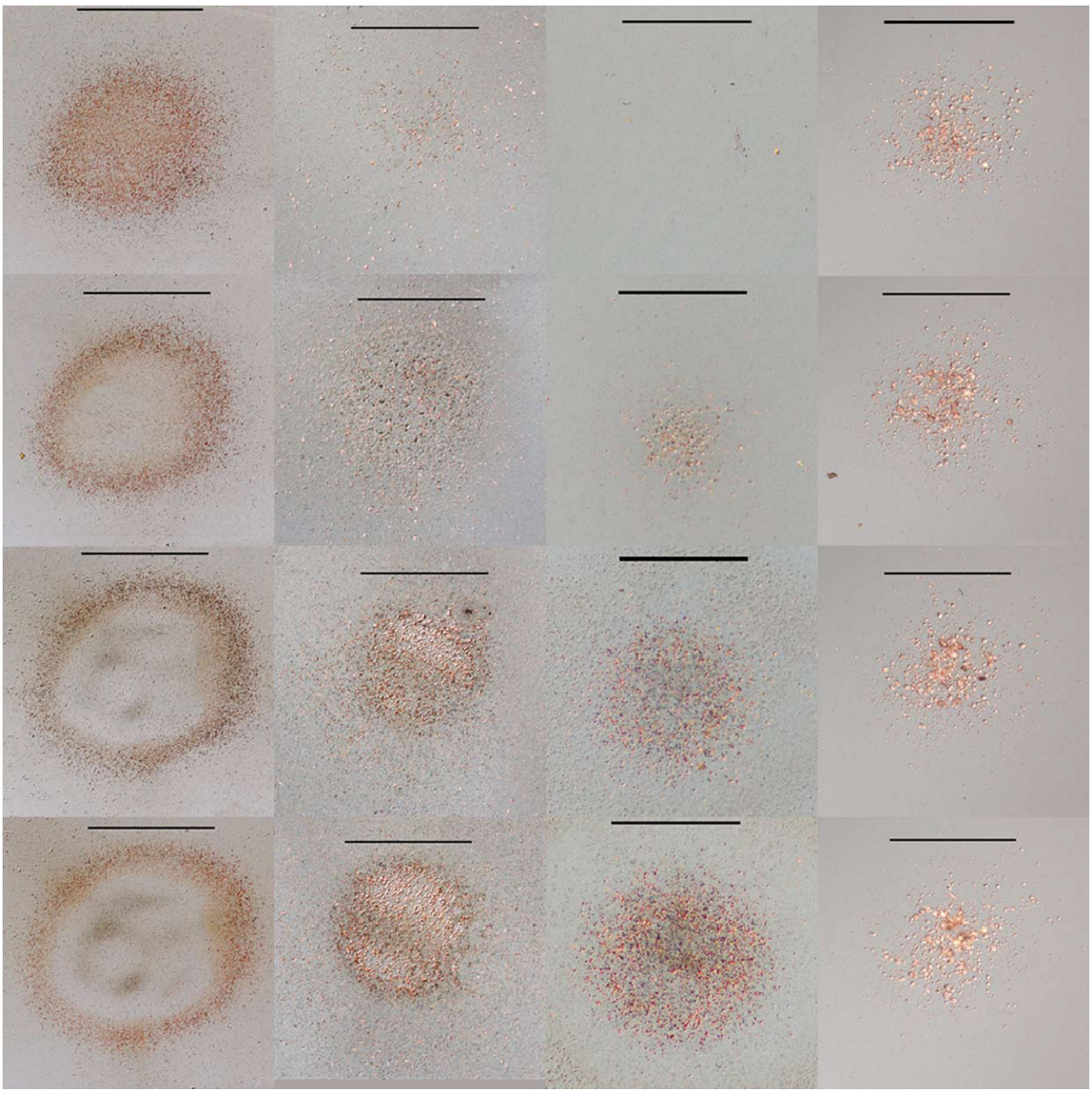

Fig. 4 LIFT transfer results (acceptor) of copper layers. Variation of laser peak fluence from top to bottom: 0.78, 1.56, 3.12, 3.9 J/cm^2. Copper donor film thickness increases from left to right: 10, 20, 30, and 60 nm. Scalebars correspond to 100 μm

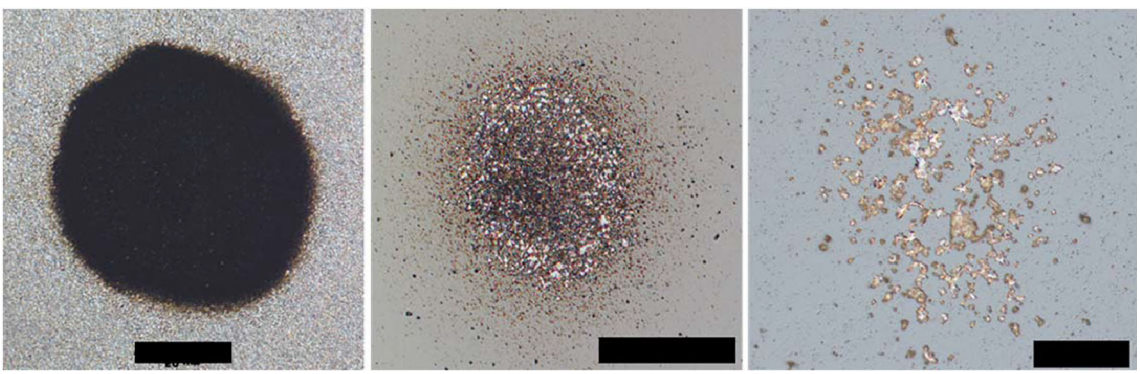

Fig. 5 Optical micrographs of LIFT results of indium films for a constant laser fluence of 7.8 J/cm^2. Left: 150 nm-thick laser-irradiated donor layer. Middle: transferred material on the acceptor side for 150 nm donor thickness. Right: transferred material on the acceptor side for 300 nm donor thickness. Scalebars correspond to 50 μm

indium layer. The 150 nm-thick donor layer is completely removed at the irradiated spot (Fig. 5, left), and the associated indium deposit appears almost homogeneous (Fig. 5, middle), while the deposit of a 300 nm-thick indium layer consists of discontinuous fragments (Fig. 5, right). Due to the fragmentation, neither the LIFT of pure copper films nor pure indium films led to satisfying results.

3.3 LIFT of combined copper–indium films

To avoid especially disintegration of transferred indium material, a copper layer was deposited on the donor glass material prior to the indium–PVD resulting in a combined copper–indium donor film. The order was chosen, because copper has a higher melting point than indium. Two parametric variations were carried out for preparing the donor films, i.e., (1) the indium layer thickness was varied for a constant copper film thickness (Fig. 6) and (2) the copper layer thickness was changed for a fixed indium film thickness (Fig. 7). It should be noted here that laser fluences in the range between 0.78 and 7.8 J/cm^2 mainly dictate the diameter of the transferred material but not the LIFT quality especially with respect to compactness. Therefore, the corresponding LIFT results are shown for a laser fluence of 7.8 J/cm^2, only.

Figures 6 and 7 demonstrate the suitability of the LIFT approach for the desired micro-island fabrication. In Fig. 6, optical micrographs of Cu–In LIFT deposits from donor layers consisting of a constant copper layer thickness of 10 nm and a varying indium layer thickness between 200 and 1000 nm are shown. The indium layer thickness is indicated in the individual micrographs. For an indium layer thickness of up to 600 nm, almost homogeneous and compact deposits are formed. An indium donor layer with a thickness beyond 600 nm leads to heterogeneous deposition. Figure 7 provides a collage of optical micrographs of LIFT deposits made of donor layers consisting of 200 nm indium films and varying copper layer thicknesses between 10 and 60 nm. In all cases, only minor disintegration of the copper–indium material is present. In contrast, for 500 nm-thick indium films with the same copper layer variation, less favorable results were obtained (see Fig. 8). Already for copper thicknesses larger than 20 nm, a trend to clumpy deposits is evident.

From variation of the z-position of the focus using optical microscopy (Nikon, software: NIS Elements, version 4.30), the thickness variation of the transferred material can be determined. This was performed on the LIFT deposit, as shown in Fig. 6, top-left (10 nm copper, 200 nm indium). The bottom part of Fig. 9 provides a 2D color map encoding the surface topography. The top part depicts a cross-sectional height profile along the horizontal line marked in the color map. The topographic maximum in this line does not exceed

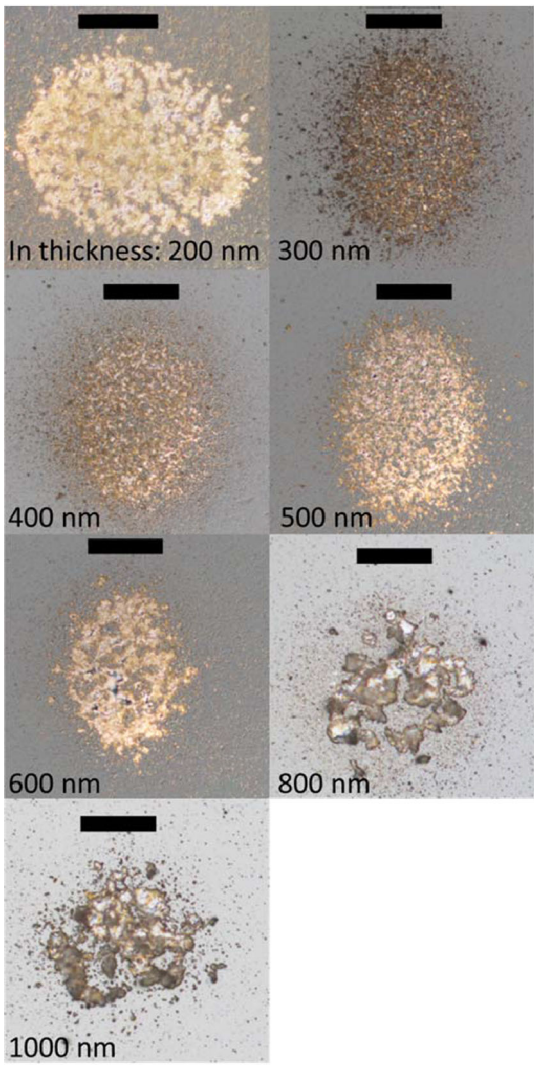

Fig. 6 Optical micrographs of LIFT results of copper–indium films for a constant laser fluence of 7.8 J/cm^2. Transferred material on the acceptor side for varying indium layer thicknesses between 200 and 1000 nm and constant copper layer thickness of 10 nm is depicted

1.5 µm. Note that the maximum thickness of the LIFT deposit significantly exceeds the thickness of the donor layer. Likely, this is due to surface tension effects in the molten deposit material. This would also explain the laterally heterogeneous material distribution across the deposit. However, the maximum height value meets the requirements for CIGSe micro-concentrator solar cell precursors. Typically, the CIGSe absorber films have a thickness of 1–2 µm. The average thickness of the deposit along the line shown in the figure is 0.74 µm ± 0.25 µm which is very close to the desired value. Expecting a thickness increase after selenization by a factor of two would result in an appropriate final thickness.

To characterize the chemical composition of LIFT deposits, EDX was used. Figure 10 shows an SEM picture

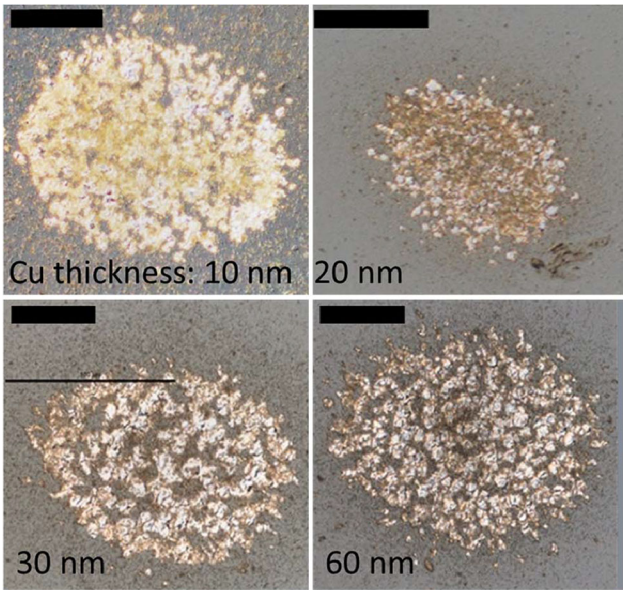

Fig. 7 Optical micrographs of LIFT results of copper–indium films for a constant laser fluence of 7.8 J/cm^2. Transferred material on the acceptor side for varying copper layer thicknesses between 10 and 60 nm and constant indium layer thickness of 200 nm is shown

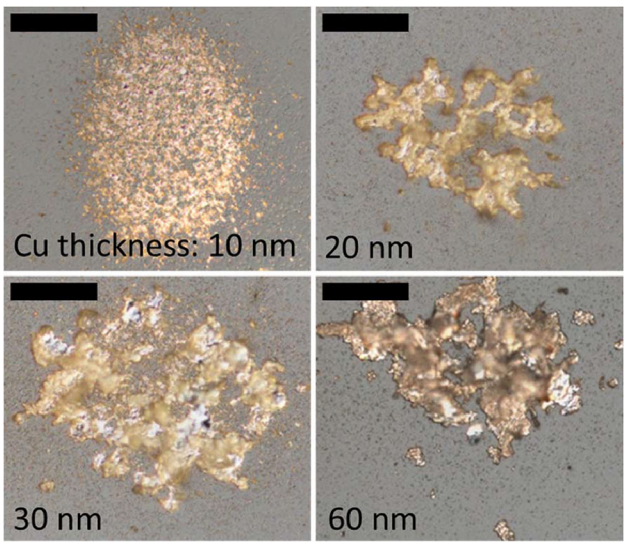

Fig. 8 Optical micrographs of LIFT results of copper–indium films for a constant laser fluence of 7.8 J/cm^2. Transferred material on the acceptor side for varying copper layer thicknesses between 10 and 60 nm and constant indium layer thickness of 500 nm is given

along with the corresponding elemental maps of copper, indium, molybdenum, oxygen, and carbon taken at a deposit (10 nm Cu, 200 nm In) produced with a laser fluence of 7.8 J/cm^2. Most strikingly, copper and indium are contained everywhere in the entire deposit. In that region, the molybdenum signal from the acceptor substrate is screened. Carbonization and oxidation are kept at a minimum.

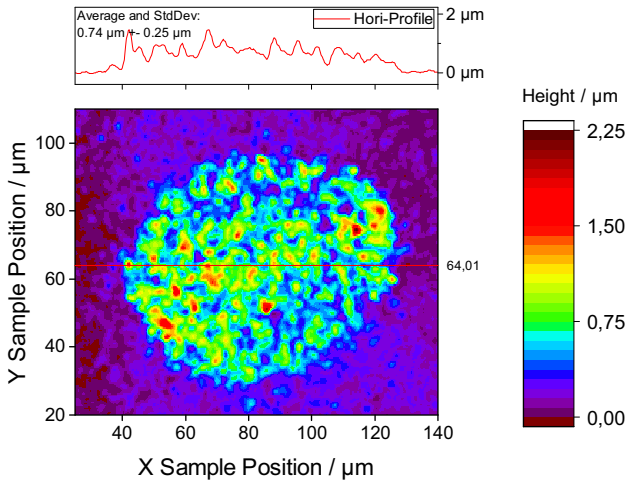

Fig. 9 Topographic details of a LIFT deposit (10 nm copper, 200 nm indium, 7.8 J/cm^2) obtained by focus variation optical microscopy. Bottom: 2D color map. Top: cross-sectional height profile along the horizontal line marked in the color map

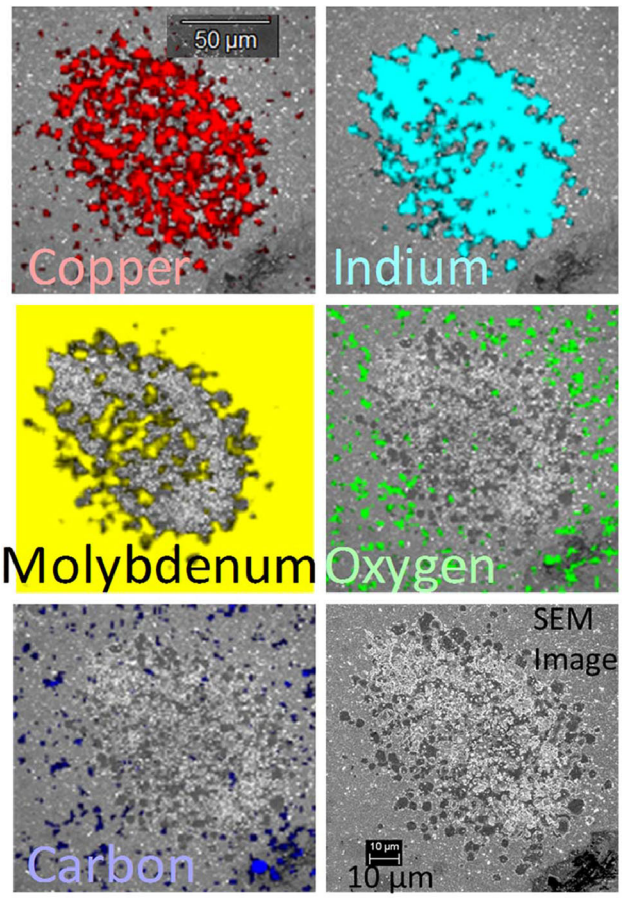

Fig. 10 EDX maps and SEM picture of a LIFT deposit (10 nm copper, 200 nm indium, 7.8 J/cm^2) on the molybdenum-coated acceptor glass sample. Elemental maps of copper, indium, molybdenum, oxygen, and carbon are presented

4 Conclusions

The CIGSe precursor materials copper and indium are suitable for femtosecond LIFT, favorably transferred using a combined copper/indium donor layer. The donor layer thickness significantly influences the quality of the LIFT deposit. EDX maps of the acceptor side prove that all materials were transferred successfully, while carbonization and oxidation are kept at a minimum. The results demonstrate a promising approach for an efficient and material saving bottom–up fabrication step of micro-concentrator solar cells.

Acknowledgements The authors would like to thank Sigrid Benemann (BAM 6.1) for the SEM/EDX measurements. The authors gratefully acknowledge financial support by the German Research Foundation (Deutsche Forschungsgemeinschaft, DFG) through BO 1129/6-1, KR 3638/3-1, and SCHM 2554/3-1.

References

1. M. Schmid, P. Manley, J. Photon Energy **5**, 057003 (2014)
2. M. Schmid, G. Yin, M. Song, S. Duan, B. Heidmann, D. Sancho-Martinez, S. Kämmer, T. Köhler, P. Manley, M.C. Lux-Steiner, J. Photon Energy **7**, 018001 (2017)
3. M. Schmid, P. Manley, Proc. SPIE **9178**, 91780K (2014)
4. M. Paire, L. Lombez, N. Péré-Laperne, S. Collin, J.-L. Pelouard, D. Lincot, J.-F. Guillemoles, Appl. Phys. Lett. **98**, 264102 (2011)
5. Zentrum für Sonnenenergie- und Wasserstoff-Forschung Baden-Württemberg, Press Release 09/2016. https://www.zsw-bw.de/en/newsroom/news/news-detail/news/detail/News/zsw-sets-new-world-record-for-thin-film-solar-cells.html. Accessed Jun 2017
6. F. Ringleb, K. Eylers, T. Teubner, T. Boeck, C. Symietz, J. Bonse, S. Andree, J. Krüger, B. Heidmann, M. Schmid, M.C. Lux-Steiner, Appl. Phys. Lett. **108**, 111904 (2016)
7. B. Heidmann, F. Ringleb, K. Eylers, S. Levcenco, J. Bonse, S. Andree, J. Krüger, T. Unold, T. Boeck, M.C. Lux-Steiner, M. Schmid, Materials Today Energy (2017) **(submitted)**
8. C.B. Arnold, P. Serra, A. Piqué, MRS Bull. **32**, 23 (2007)
9. P. Delaporte, A. Ainsebaa, A.-P. Alloncle, M. Benetti, C. Boutopoulos, D. Cannata, F. Di Pietrantonio, V. Dinca, M. Dinescu, J. Dutroncy, R. Eason, M. Feinaugle, J.-M. Fernández-Pradas, A. Grisel, K. Kaur, U. Lehmann, T. Lippert, C. Loussert, M. Makrygianni, I. Manfredonia, T. Mattle, J.-L. Morenza, M. Nagel, F. Nüesch, A. Palla-Papavlu, L. Rapp, N. Rizvi, G. Rodio, S. Sanaur, P. Serra, J. Shaw-Stewart, C.L. Sones, E. Verona, I. Zergioti, Proc. SPIE **8607**, 86070Z (2013)
10. A. Piqué, R.C.Y. Auyeung, H. Kim, N.A. Charipar, S.A. Mathews, J. Phys. D Appl. Phys. **49**, 223001 (2016)
11. P. Delaporte, A.-P. Alloncle, Opt. Laser Technol. **78**, 33 (2016)
12. I. Zergioti, S. Mailis, N.A. Vainos, P. Papakonstantinou, C. Kalpouzos, C.P. Grigoropoulos, C. Fotakis, Appl. Phys. A **66**, 579 (1998)
13. R. Fardel, M. Nagel, F. Nüesch, T. Lippert, A. Wokaun, Appl. Surf. Sci. **254**, 1322 (2007)
14. A. Palla-Papavlu, M. Dinescu, A. Wokaun, T. Lippert, Appl. Phys. A **117**, 371 (2014)
15. C.B. Arnold, A. Piqué, MRS Bull. **32**, 9 (2007)
16. L. Rapp, C. Constantinescu, Y. Larmande, A.K. Diallo, C. Videlot-Ackermann, P. Delaporte, A.P. Alloncle, Sens. Actuators A **224**, 111 (2015)
17. P. Serra, J.M. Fernández-Pradaz, M. Colina, M. Duocastella, J. Domínguez, J.L. Morenza, J. Laser Micro Nanoeng. **1**, 236 (2006)
18. A. Palla-Papavlu, T. Lippert, M. Dinescu, Rom. Rep. Phys. **63**, 1285 (2011)
19. M. Nagel, T. Lippert, Laser-induced forward transfer for the fabrication of devices, in *Nanomaterials; processing and characterization with lasers*, ed. by H. Zeng, C. Guo, W. Cai, S.C. Singh (Wiley, Weinheim, 2012), pp. 255–316
20. B. Hopp, T. Smausz, N. Kresz, N. Barna, Z. Bor, L. Kolozsvári, D. Chrisey, A. Szabó, A. Nógrádi, Tissue Eng. **11**, 1817 (2004)
21. J. Shaw Stewart, T. Lippert, M. Nagel, F. Nüesch, A. Wokaun, AIP Conf. Proc. **1278**, 789 (2010)
22. I. Zergioti, A. Karaiskou, D.G. Papazoglou, C. Fotakis, M. Kapsetaki, D. Kafetzopoulos, Appl. Phys. Lett. **86**, 163902 (2005)
23. Z. Kántor, Z. Tóth, T. Szörényi, Appl. Surf. Sci. **86**, 196 (1995)
24. M.V. Shugaev, N.M. Bulgakova, Appl. Phys. A **101**, 103 (2010)
25. J.A. Grant-Jacob, B. Mills, M. Feinaeugle, C.L. Sones, G. Oosterhuis, M.B. Hoppenbrouwers, R.W. Eason, Opt. Mater. Express **3**, 747 (2013)
26. R. Pohl, C.W. Visser, G.-W. Römer, D. Lohse, C. Sun, B. Huis in't Veld, Phys. Rev. Appl. **3**, 024001 (2015)
27. J. Thomas, R. Bernard, J.T. Thomas, K. Alti, S. Chidangil, S. Kumari, A. Khare, D. Mathur, Laser Part. Beams **32**, 55 (2013)
28. K. Alti, S. Dwivedi, S. Chidangil, D. Mathur, A. Khare, Laser Part. Beams **33**, 449 (2015)
29. L. Yang, C.-Y. Wang, X.-C. Ni, Z.-J. Wang, W. Jia, L. Chai, Appl. Phys. Lett. **89**, 161110 (2006)
30. Y. Li, W. Ching-Yue, Chin. Phys. B **18**, 4292 (2009)
31. M. Zenou, A. Sa'ar, Z. Kotler, Small **11**, 4082 (2015)
32. M. Zenou, Z. Kotler, Opt. Express **24**, 1431 (2016)
33. C.W. Visser, R. Pohl, C. Sun, G.-W. Römer, B. Huis, B. Huis in't Veld, D. Lohse, Adv. Mater. **27**, 4087 (2015)
34. Application data sheet: mechanical properties of copper and copper alloys at low temperatures, Copper Development Association Inc., New York, NY. https://www.copper.org/resources/properties/144_8/. Accessed June 2017
35. R.P. Reed, C.N. McCowan, R.P. Walsh, L.A. Delgado, J.D. McColskey, Mat. Sci. Eng. A **102**, 227 (1988)
36. N. Orbey, G.A. Jones, R.W. Birkmire, T.W.F. Russell, J. Phase Equilib. Sect. I Basic Appl. Res. **21**, 509 (2000)
37. J.M. Liu, Opt. Lett. **7**, 196 (1986)
38. S. Martin, PhD Thesis. Freie Universität, Berlin (2004)
39. P.B. Johnson, R.W. Christy, Phys. Rev. B **6**, 4370 (1972)
40. N. Tsakiris, K.K. Anoop, G. Ausanio, M. Gill-Comeau, R. Bruzzese, S. Amoruso, L.J. Lewis, J. Appl. Phys. **115**, 243301 (2014)
41. C.M. Rouleau, C.Y. Shih, C. Wu, L.V. Zhigilei, A.A. Puretzky, D.B. Geohegan, Appl. Phys. Lett. **104**, 193106 (2014)